ELSEVIER

Composites: Part A 32 (2001) 1379–1394

composites
Part A: applied science and manufacturing

www.elsevier.com/locate/compositesa

Textile composites: modelling strategies

S.V. Lomov[a,1,*], G. Huysmans[a], Y. Luo[a], R.S. Parnas[a,2], A. Prodromou[a], I. Verpoest[a], F.R. Phelan[b]

[a]*Department Metallurgy and Materials Engineering, Katholieke Universiteit Leuven, de Croylaan 2, B-3001 Heverlee, Belgium*
[b]*Polymers Division, NIST, Gaithersburg, USA*

Abstract

Textile materials are characterised by the distinct hierarchy of structure, which should be represented by a model of textile geometry and mechanical behaviour. In spite of a profound investigation of textile materials and a number of theoretical models existing in the textile literature for different structures, a model covering all structures typical for composite reinforcements is not available. Hence the challenge addressed in the present work is to take full advantage of the hierarchical principle of textile modelling, creating a truly integrated modelling and design tool for textile composites. It allows handling of complex textile structure computations in computer time counted by minutes instead of hours of the same non-linear, non-conservative behaviour of yarns in compression and bending. The architecture of the code implementing the model corresponds to the hierarchical structure of textile materials. The model of the textile geometry serves as a base for meso-mechanical and permeability models for composites, which provide therefore simulation tools for analysis of composite processing and properties.

Keywords: Textile reinforcements; B. Mechanical properties

1. Introduction

Reliable prediction of properties (and mechanical behaviour in the more broad sense) of composite materials is of the primary importance for the success of usage of textile composites. The complexity of the structure and the presence of a hierarchy of structural and scale levels (10^{-5} m-fibres, 10^{-3} m-yarns/tows, 10^{-1} m-fabrics, 10^{0} m-composite parts) lead to a high complexity of the predictive models, a high level of approximation in them, and to the high level of uncertainty of the predictions, when errors are accumulated when the model progresses from one hierarchical level to another. On the other hand, the same hierarchy provides a very generic and reasonable route for construction of the predictive models, which is the subject of this paper. It continues publications of the present authors on the concept of Textile Geometry Preprocessor for the simulation of composites processing and mechanical behaviour [1–7].

Textiles are hierarchically structured fibrous materials. As it was discussed in the classical paper of Hearle et al. [8], this description of the nature of textiles defines an efficient approach to the construction of mathematical models of the geometry and the mechanical behaviour of textile structures. After more than 60 years of work creating textile structural models, the hierarchical approach has never been fully utilised, despite its recognised usefulness and, perhaps, necessity. During the 30s, the first serious mechanical treatments of the structure of textile materials were published by Peirce [9] (almost unknown in the English literature, Russian contributions by Pozdnyakov [10] and Novikov [11] should also be cited here). Since then, the stream of papers dedicated to the mechanical description of textile structures was constant and resulted in a comprehensive treatment on 'Mechanics of Flexible Fibre Assemblies' in 1980 [12]. In the following years, the ideas and generic approaches outlined in this book were pursued further. The state-of-art of textile mechanics in the beginning of the 21st century includes models of the internal geometry of the basic textile structures, such as continuous-filament and staple yarns, random fibre mats, and woven and knitted structures.

Nevertheless, these models deal primarily with a particular structure (e.g. a plain weave or a rib knit). There is a lack of generalised models (e.g. a model of a woven fabric, in which the weave pattern itself enters as a parameter). The other drawback is the lack of models that combine two hierarchical levels. An example application, which asks for such a combined model is the problem of fabric

* Corresponding author. Fax: +32-1632-1990.
E-mail address: stepan.lomov@mtm.kuleuven.ac.be (S.V. Lomov).
[1] On leave of absence from St.-Petersburg State University of Technology and Design, Russia.
[2] On leave of absence from Institute of Materials Science, University of Connecticut, Storrs, USA.

1359-835X/01/$ - see front matter
PII: S1359-835X(01)00038-0

permeability: a suitable model should include a description of both the macro-porosity (i.e. between the yarns) and the micro-porosity (i.e. between the fibres in a yarn) [13].

The hierarchical approach of a geometry model architecture is naturally implemented via the minimum energy principle (MEP), introduced by Hearle and Shanahan [14] and de Jong and Postle [15]. This principle allows the decomposition of a problem into a set of problems for structural elements, leading to physically sound and computationally feasible models. There are two questions connected with the use of a MEP in textiles. One is the heuristic nature of the principle itself when applied to non-conservative mechanical systems — like textiles. This question has not been solved so far, and results obtained with the help of the MEP will always remain a kind of approximation of the behaviour of the real textile structure. The second question relates to the application of the MEP to textiles where the textile structure enters the problem as a parameter. As it will be shown below, MEP provides a quite straightforward way to do this, but has not been explored so far.

The results of the geometrical modelling serve as crucial input to the models of composites processing and mechanical behaviour. In the permeability module, the three-dimensional permeability tensor is calculated, and serves as a preprocessor for any flow modelling or mould filling software. The main advantage is that local variations in textile geometry, and hence in permeability, can be taken into account in an explicit way. In the meso-mechanics module, the thermo-mechanical properties of the composite representative volume element are calculated. Different meso-mechanical modelling options are available. They all result in a prediction of the three-dimensional homogenised stiffness matrix, but also allow the calculation of local stresses, strains and damage under any external loading.

Hence the composite material, as the final product in the sequence 'fibre → yarn → textile → preform → composite', is included in the hierarchical description of the 'textile world', taking full advantage of the versatility of this approach.

2. Hierarchy of the textile composite structure

Table 1 shows the 'staircase' of structural elements of a textile composite and modelling problems associated with each scale/structure level. The useful 'rule of thumb' for the model is to avoid unnecessary mixture of hierarchical levels: use yarn, not fibre, properties to predict behaviour of a fabric. Each level on the staircase is occupied by models, which use the input data of topology and spacing parameters of structural elements (i.e. weave pattern and warp/weft count) and properties of the elements themselves (i.e. yarns in a fabric) to predict properties of the structure (i.e. geometry of the fabric). If necessary, data from the lower level are introduced (i.e. fibrous structure of yarns in the fabric).

The modern *Object Oriented Programming* (*OOP*) technique is ideally suited to implement the hierarchical nature of textiles. The three main features of the OOP are *encapsulation*, *inheritance*, and *polymorphism*.

Encapsulation means that the *object* holds not only data, but also the behaviour. Applying this to a *Yarn* object, we can consider the data fields and *methods* (procedures describing the object behaviour) shown in Table 2. Wherever the Yarn object will be encountered in the software, all these data fields and methods will be accessible, and the model can instruct the yarn, say to *Compress* under the force *Q*. One can say that the Yarn object virtually represents the actual yarn. Note that the Yarn object does not contain fibre data. It is designed to be sufficient for geometrical calculations on the 'yarn–fabric' level of the textile hierarchy.

Inheritance means that one can construct another object, say *YarnWithFibreData* (Table 2), which will *inherit* all the data and the behaviour of the parent Yarn object, but adds fibre data and behaviour, which in its turn is encapsulated in the *Fibre* object, placed on the lower level of the structural hierarchy. Now it is possible not only to evaluate the yarn properties using the fibre data and a structural model of the yarn, but also to determine properties lying on a lower hierarchical level (i.e. the fibrous structure of the yarn). The new object virtually represents the actual yarn with some added knowledge. The inheritance feature of the OOP provides therefore a logical basis for the gradual improvement of the model.

Polymorphism gives the developer the possibility to take full advantage of this gradual improvement process.

Table 1
Hierarchy of structure and models of a textile composite

Structure	Elements	Models
Yarn (tow)	Fibres	Fibre distribution in the yarn and its change under load/strain Mechanical properties of the yarn
Fabric (woven, knitted…)	Yarns	Geometry of yarns in the fabric and its change under load/strain Mechanical behaviour of the fabric repeat under complex loading
Composite unit cell	Fabric Matrix	Mechanical properties (stiffness matrix/non-linear; strength) Permeability tensor
Composite part	(Deformed) unit cells	Behaviour under loading Flow of the resin Behaviour in the forming process

Table 2
Fibre and Yarn objects as implemented in software via OOP approach

Object	Data		Methods
	Group	Fields	
Fibre	General	Name	
		Linear density, tex	
		Diameter, mm	
		Density, g/cm^3	
	Mechanics	Longitudinal Young modulus, Gpa	
		Longitudinal Poisson ratio	
		Transverse Youngs modulus, Gpa	
		Transverse Poisson ratio	
		Longitudinal shear modulus, Gpa	
		Transverse shear modulus, Gpa	
		Tenacity, Mpa	
		Ultimate elongation	
Yarn	General	Name	Compute mass for a given length
		Yarn type: monofilamnet, continuous filament or spun	
		Linear density, tex	
	Geometry of the cross-section	Assumed shape: elliptical or lenticular or rectangular	Compute volume of the given yarn length
		Dimensions of the cross-section in the free state d_{01}, d_{02}, mm	Determine, whether the given point (x,y) (co-ordinates on the plane of the cross-section) lies inside the yarn
	Compression	Type of compression behaviour: no compression, 'locked' compression in a textile structure or compression law given	Compute compressed yarn dimensions under a given force per unit length
		Compression coefficient $\eta_1 = d_1/d_{10}$ as a value or a function of compressive force Q per unit length	Compute compression of two intersecting yarns for a given normal force and angle of intersection
		Flattening coefficient $\eta_2 = d_2/d_{20}$ as a value or a function of compressive force Q per unit length	
	Bending	Bending curve 'torque-curvature' (linear for the constant bending rigidity) $M(\kappa)$	Compute bending rigidity value B for a given curvature
	Friction	Friction law yarn–yarn in the form $F = fN^n$, where N is a normal force	Compute friction force for a given normal force
Yarn with fibre data	inherits data and methods of Yarn, adds the following and replaces (shown in **bold**) some of Yarn methods		
	General	Twist, 1/m	Compute the twist angle
		Twist direction (S or Z)	Compute linear density from fibre data
	Fibre	Fibre data (Fibre object)	Compute fibrous content and fibre direction in the vicinity of the given point (x,y). Fibrous content is assumed constant inside a yarn
		Number of fibres in cross-section	
		Fibre distribution in the yarn	
	Compression		Compute compressed yarn dimensions under a given force per unit length **and fibre distribution in it**
	Bending		Compute bending resistance from fibre data

Consider a method Compress, which for the Yarn object simply computes the cross-sectional dimensions in the compressed configuration, but which for the Yarn with fibre data object additionally computes the fibre distribution in the compressed state. When used inside the software in reference to a certain Yarn object, the method will be applied in the former style if the object does not contain fibre data, and in the latter style, if fibre data are present. The Yarn object will be polymorph, changing its behaviour according to its actual contents.

The OOP approach provides a powerful tool for the construction of 'virtual textiles', and will be employed in full below.

3. Level I. Fibre → yarn: fibrous structure and mechanical properties of a yarn

The geometry of a textile structure in the relaxed state (i.e. in absence of external forces) is determined by the

equilibrium of the yarn interaction forces, which naturally arise to accommodate the topology of the yarn contacts within the textile. Bending of the yarns — necessary to maintain the topology — creates transversal forces at the yarn contacts. These forces lead to yarn compression and flattening and — in case of non-symmetrical contact conditions — to local deflections of the yarn path from the ideal directions, which are in turn resisted by friction between the yarns). In the relaxed state the yarns are free of tension. The weaving process does not imply torsion of the yarns; for knitted fabrics however torsion takes place.

Therefore, the following yarn properties should be included in the input data for the geometrical model.

3.1. Linear density and dimensions of the yarn in the free state

The linear density of a yarn has a certain unevenness. An interesting route for the development of geometrical models would therefore be to include stochastic effects and to explore the influence of the yarn unevenness on the fabric geometry. However, this has not been done so far.

The shape of the yarn cross-section in the free state is normally assumed to be circular or elliptical (e.g. in the case of sized glass rovings for composite reinforcements). The diameter of the yarn is usually computed with the formula

$$d_0 = C\sqrt{T}, \tag{1}$$

where d_0 is the yarn diameter, T is the linear density and C is an empirical coefficient, taking into account the fibre density, fibre twist and fibre packing within the yarn. It should be clearly understood that Eq. (1) and the concept of a diameter of the yarn with a distinct 'border' is itself are approximations as the fibrous structure of the yarn on the yarn-fabric level within the textile hierarchy is neglected [16]. Fig. 1 illustrates the nature of this approximation.

3.2. Compression of yarns

Compression of yarns causes a change of the yarn cross-sectional dimensions within the fabric and directly affects the fabric geometry. Standard equipment (KES-F) allows measuring the compressive deformation of the yarn as a function of the applied force per unit length of the yarn (Fig. 2)

$$d_1 = d_{10}\eta_1(Q), \tag{2}$$

where d_1 is the compressed dimension of the yarn in the direction of the compressive force Q, d_{10} is the corresponding dimension in the free state, and η_1 is an empirical function.

A number of problems arise in the experimental characterisation of the compressive behaviour of yarns

1. The first problem is the necessity to measure not only the compressive (in the direction of the force), but also the spreading (in the direction perpendicular to the force) deformation of the yarn (Fig. 2)

$$d_2 = d_{20}\eta_2(Q), \tag{3}$$

where d_2 is the compressed dimension of the yarn in the direction normal to the compressive force Q, d_{20} is the corresponding dimension in the free state, and η_2 is an empirical function. The standard KES-F equipment does not provide any information about yarn spreading. The solution may be to use a specialised experimental rig, proposed in Ref. [17], or to use approximate empirical relationships between η_2 and η_1, as introduced in Refs. [18–20].

2. The values of d_{10} and d_{20} are an approximation of the yarn cross-sectional dimensions in the free state, as the exact cross-section is not clearly defined. A special routine for the processing of the experimental data has been proposed in Ref. [21].

3. Even if the functions Eqs. (2) and (3) are known, their application is complicated by the interaction effects of crimped yarns. Kawabata [22] proposed a special device for the investigation of the compression behaviour in this situation. However, too many independent variables enter the experiment (yarn crimp, angle of yarn intersection, compressive force), and the measurement method mixes compressive and bending deformation of yarns. Hence, this technique cannot be considered as standard to obtain the necessary input data for the fabric geometry models. The use of experimental data obtained on 'flat' compressive equipment is therefore not a straightforward exercise and asks for some approximate treatment when the yarns are crimped.

4. The KES-F measurement provides data for a laterally unconstrained compression. For sparse textile structures this is sufficient, but in the case of a dense structure either the constrained compression should be studied, or some mechanical model should be introduced. The former does not seem feasible because of the many variables involved. The latter leads to a description of the yarn behaviour on a lower hierarchical level, namely the fibre-yarn level.

3.3. Bending and torsion of yarns

The bending and torsion behaviour of yarns has been studied extensively and the standard equipment to measure it is present (KES-F for bending and a torsion rig as described for example in Ref. [23–25]). This behaviour is non-linear, but as a first estimate it can be approximated by a linear behaviour with constant bending and torsion rigidities B and C. An important and still unanswered question is the influence of bending and torsion behaviour upon yarn compression (caused by a change of the cross-sectional shape and the redistribution of the fibres inside the yarn).

4. Level II. Yarn → fabric

Here we shall provide some examples of models of textile structures at the hierarchical level 'Yarn → Fabric'.

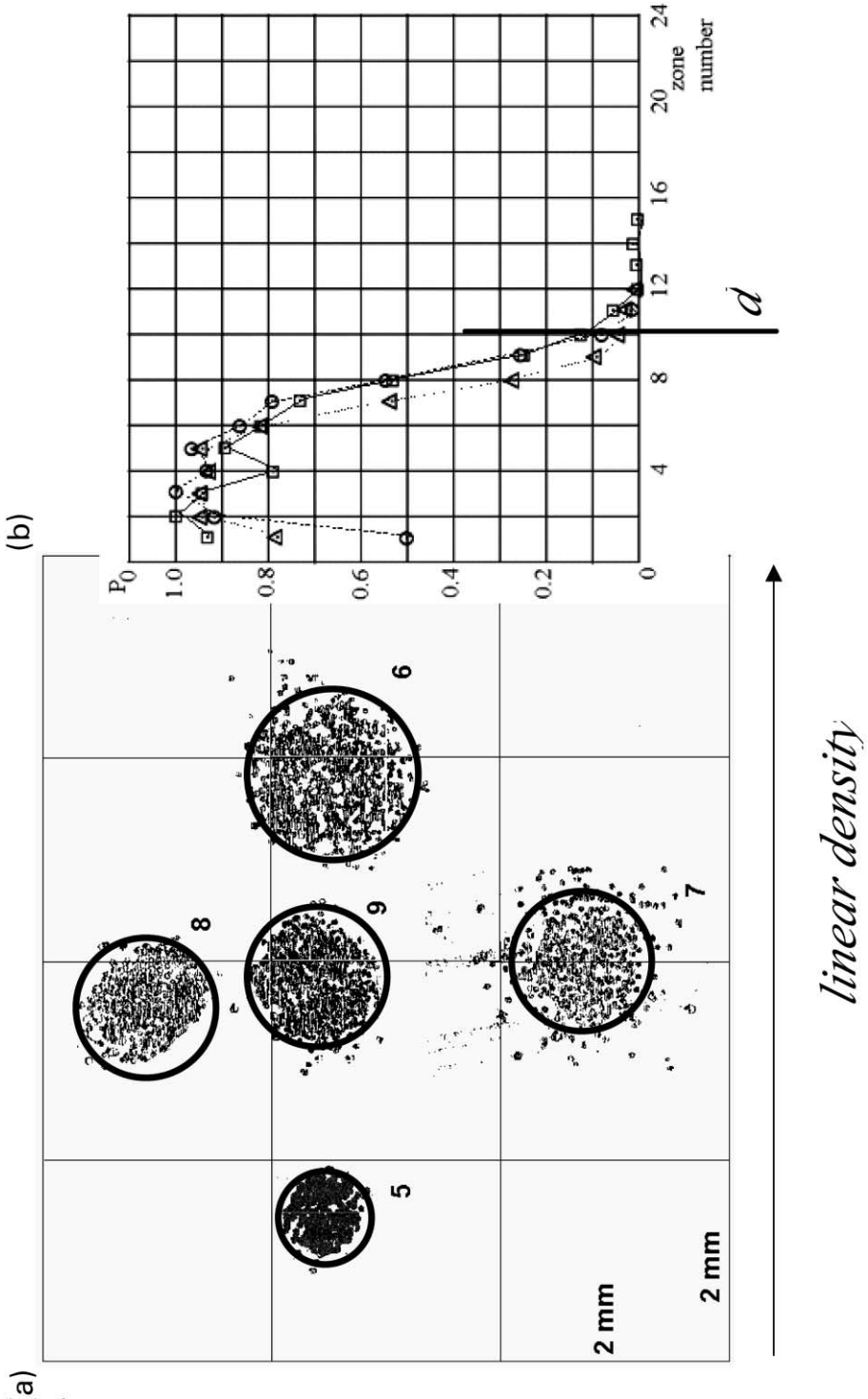

Fig. 1. (a) Actual fibrous structures of acrylic yarns of different linear density and twist and their diameters computed with Eq. (1); (b) distribution of fibres over the radial zones of the yarn cross-section and the diameter computed with Eq. (1).

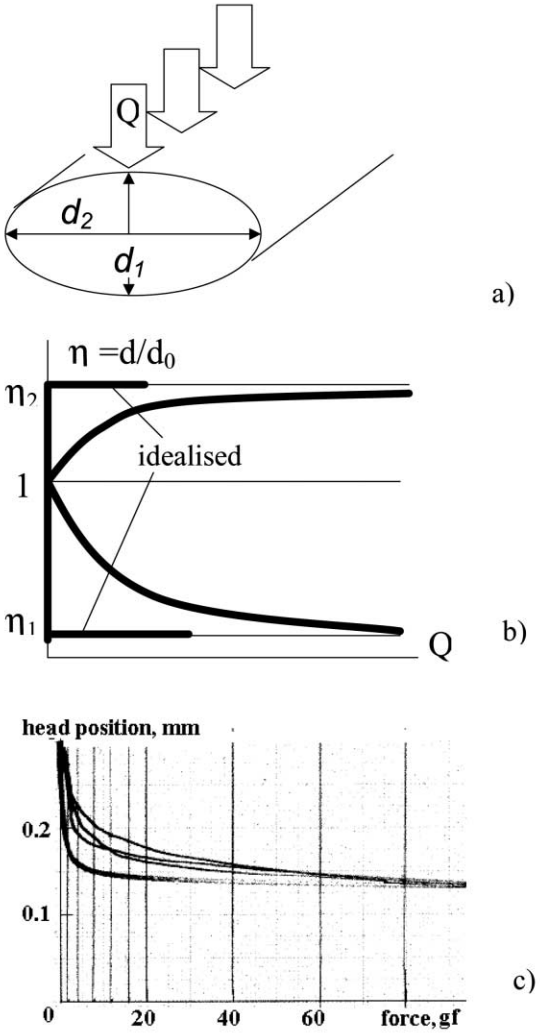

Fig. 2. Compression of fibres: (a) loading scheme; (b) typical compression diagram and a 'locked' approximation; (c) typical KES-F measurement (glass roving 480 tex).

4.1. Internal geometry of a woven fabric

We shall consider here a woven fabric. The model is extensively described elsewhere [26,1,2], here we give just a brief description. Consider a single repeat of the fabric. Assume further as given: (1) all the necessary yarn properties; (2) the topology of the yarn interlacing pattern within the fabric repeat; (3) the yarn spacing within the repeat (i.e. the mean distance between warp/weft yarns in a woven fabric or the course/wale spacing in weft-knitted fabrics). The problem is to compute the spatial placement of all yarns in the repeat. In more practical terms, this means: determine all the yarn heart-lines within the repeat and define the yarn cross-sectional shape and its dimensions normal to the yarn heart-line for each point along the yarn heart-lines.

The list of the necessary yarn properties includes yarn geometry in free state and its behaviour in compression, bending and friction. These data are not readily found in a yarn specification, but can be measured on the standard textile laboratory equipment, or predicted if a model of the previous hierarchical level Fibre → Yarns is available. Topology of the yarn interlacing inside a multi-layered woven structure is described using a matrix coding algorithms [27]. It allows decomposition of yarns in the unit cell into elementary crimp intervals, which leads to a system of algebraic equations representing the minimum energy configuration of the yarns. Solution of the equations gives heights of out-of-plane and in-plane crimp of warp and weft yarns, and the complete yarn geometry is then reconstructed with the help of a spline approximate solution for the minimum energy problem on each crimp interval. This algorithm is implemented in the *WiseTex* software (Figs. 3–5).

Once the geometrical model of a fabric is built, the model of fibre distribution inside yarns can be used to produce a complete description of the unit cell fibrous structure. In the simplest case such a model assumes even distribution of fibres, taking into account yarn compression inside the fabric. Alternatively, more complex models of fibre distribution can be employed. The result can be expressed in two ways: Yarn Path Mode and Fibre Distribution Mode. The former uses a description of spatial placement of yarns in the unit cell. The latter mode generates fibre volume fraction V_f and the direction of fibres for any point inside the unit cell. The value of V_f can be zero if the point does not lie inside a yarn. These two types of output data constitute the input for the meso-mechanical models of composites, which are described below.

4.2. Topology of the weft-knitted fabric

We shall use here an approach to code a weft-knitted structure described in Ref. [28]. Weft-knitted structures can be constructed from a small set of basic building blocks, or stitches, defined by the individual needle actions. These blocks or stitches are interconnected according to the number and the spatial arrangement of the needle beds. For a double bed structure, we can schematically represent a basic loop structure (Fig. 6a, left) and its possible interlacing patterns (Fig. 6a, right).

The three possible loop configurations for a weft-knitted structure are respectively the plain stitch, the tuck stitch and the float or miss. They can all be represented in a similar scheme (Fig. 6b), which consequently provides a basis for the topological description of the fabric structure.

In order to link the individual loop patterns of Fig. 6b into a coherent structure, the number of needle beds needs to be taken into account together with the needle bed gating. In the present work, we will demonstrate both the rib and the interlock gating. For the rib gating, loops are alternatively formed on the front and back needle beds. Front and back loops align in columns along the wale direction of the fabric. From a machining viewpoint, the needles of the two beds have a zero relative offset in the course direction, but are

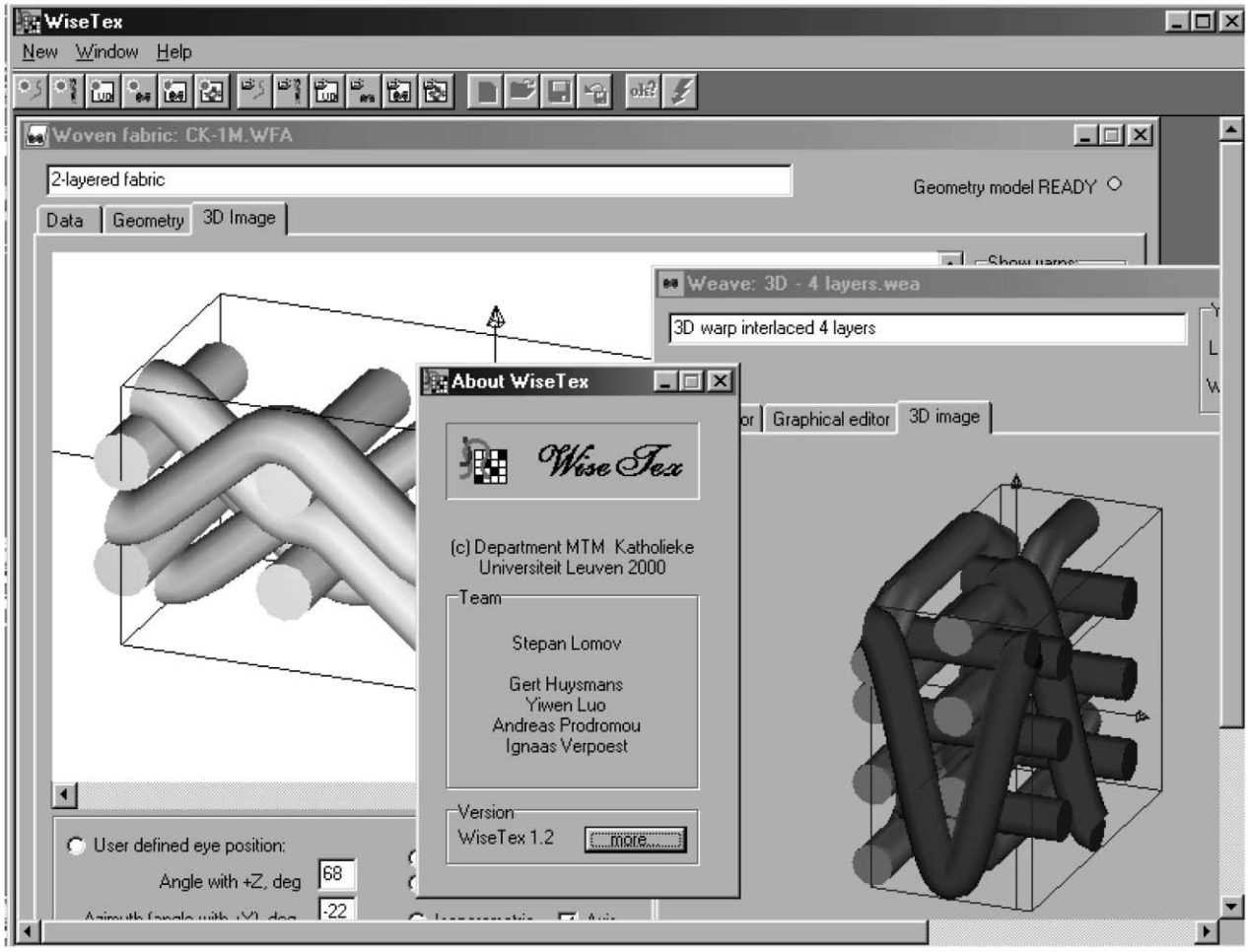

Fig. 3. WiseTex software.

positioned in between each other along the wale direction. Therefore, we can combine front and back needles into pairs (tracks) that are arranged in a two-dimensional matrix as indicated in Fig. 7a.

In the interlock configuration, front and back needles are aligned along the course direction. Interlock fabrics can be regarded as two separate fabrics knitted on the individual needle beds, but where the threads from the back bed are transferred to the front bed at the interlock positions and vice versa. The tracks are now arranged in a vertical direction as shown in Fig. 7b.

The topology for weft-knitted structures can now be described by a combination of a matrix coding and the gating configuration. Each matrix entry represents an individual needle action and is a combination of two pieces of information: (1) the position of the needle (F or B) and (2) the stitch type (X or O for a plain stitch on respectfully front or back bed, +for a tuck stitch and *blank* for a miss or float). From the topology it is always possible to create the interlacing sequence of the yarns in the fabrics. Fig. 8 gives some examples for the single jersey, rib- and interlock gating, respectively, together with the topological code.

From the examples in Fig. 8 it becomes obvious that the number of interlacing points in knit structures (constituting the end points of the structural elements) is not only a function of the stitch type itself, but also from the specific way in which the stitches from the different needle beds are connected. This information is implicitly contained in the schemes of Fig. 8, hence they are more convenient to use than a coding which would be based on an explicit identification of the contact points between the yarns.

4.3. Deformation of a dry fabric: compression

Modelling of deformation of a dry fabric is the necessary part of any predictive model of preform formability. We consider here the case of compression of a woven fabric [21].

When a fabric is compressed, the following changes in geometry take place: (1) warp and weft yarns are compressed; (2) the less crimped yarn system increases its crimp and vice versa. The latter process is due to additional bending forces resulting from interaction of more crimped (and therefore higher) parts of yarns with the compressing

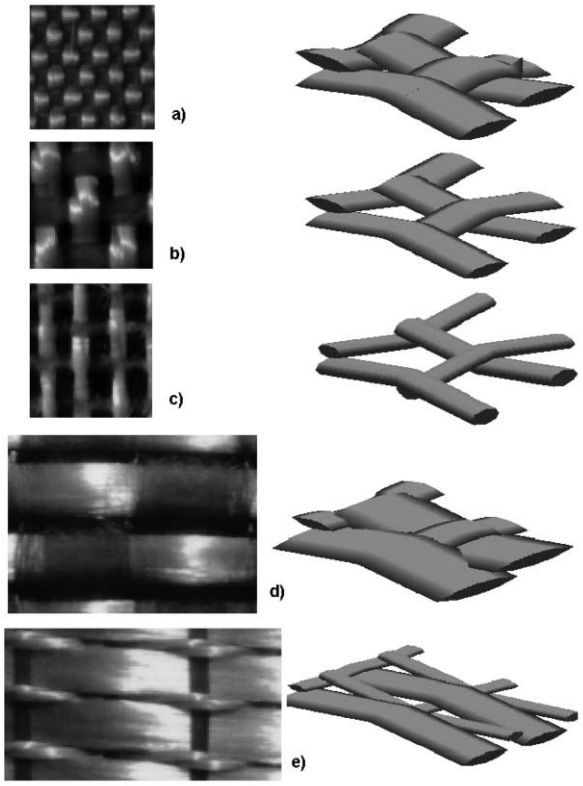

Fig. 4. Photographs (left) and computed images (right) of different types of 2D glass reinforcements: (a–c) glass multy-filaments, different weave density; (d) glass rovings; (e) unidirectional weave.

surface. To compute the compression of yarns we use the known (measured on the Kawabata textile testing equipment) compression law of individual yarns and assume an even distribution of the compressive pressure over the fabric surface. The change of crimp is computed from the energy balance: *work of compressive force on change of thickness = change of bending energy of yarns*. The model, therefore, uses the same methodology as the model of internal geometry of yarns described above. Fig. 9 demonstrates the comparison of the predicted and experimental compression curves for a glass reinforcement.

4.4. Deformation of a dry fabric: tension, shear, bending

The same approach can be applied for tension (bi- and uni-axial) of a woven fabric. Applied strain increases spacing of yarns in the fabric. Crimp heights in the deformed state are computed via the energy balance between work of transversal forces on change of crimp heights of warp and weft and change of bending energy of yarns. Strain of yarns in crimp intervals are then computed and forces evaluated using a non-linear tension diagram of the yarn. Fig. 10 illustrates the output of the tension model.

Similar approach can be applied to shear and bending of the fabric [20,29].

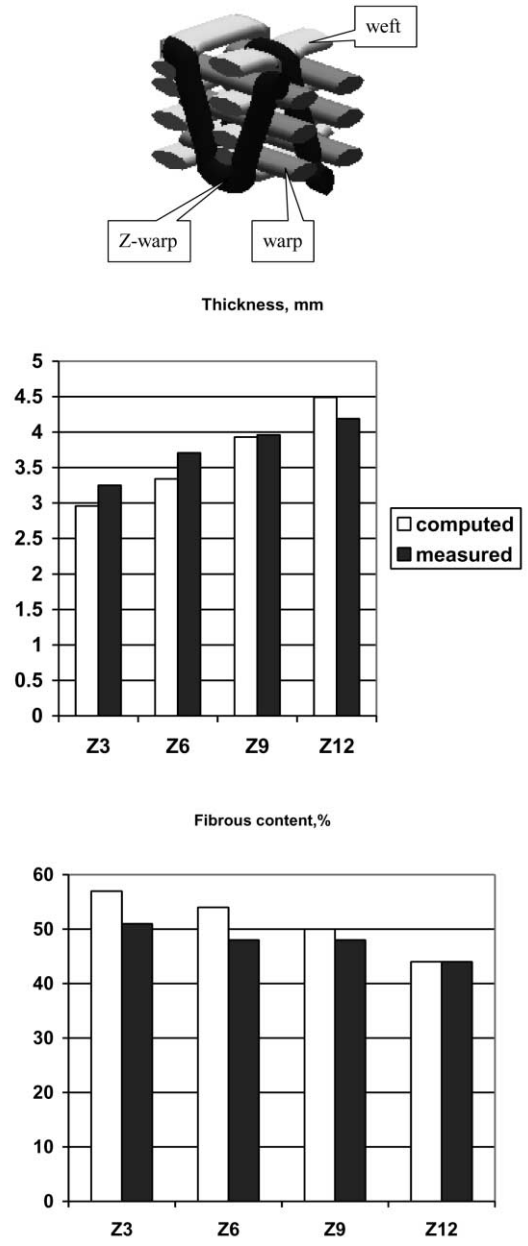

Fig. 5. Measured and computed properties of 3D carbon fabrics studied in Ref. [38].

5. Level III. Fabric → unit cell of the composite

The textile geometry and mechanics models described in the previous section, provide a tool — Textile Geometry Preprocessor (TGP) — to generate an input data representing the internal geometry of a textile. These data are used to simulate mechanical properties and permeability characteristics of the unit cell of the textile composite, as shown in the Fig. 11.

5.1. Meso-mechanical model

Apart from solid finite element models, meso-mechanical

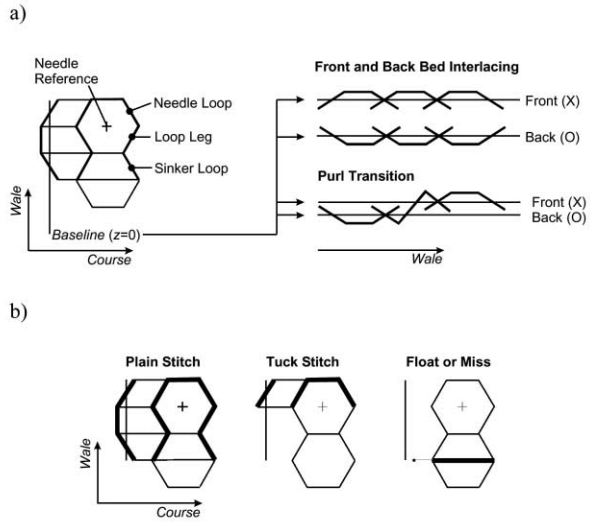

Fig. 6. (a) Schematic loop structure and interlacing pattern for double jersey weft-knit; (b) basic stitch types in a weft-knitted structure.

models for textile composites basically require one of two distinct, idealised geometrical input formats. Accordingly the TGP provides two different modes of representing textile unit cell geometry as meso-mechanical model input (Figs. 12 and 13).

A first series of models uses the actual yarn co-ordinates to derive the reinforcement volume fraction, orientation distribution, yarn shape and curvature, depending upon the model complexity. To be capable for providing the necessary geometrical input needed by these models, the *Yarn Path Mode* (YP) has been developed. In the Yarn Path mode TGP stores geometry of paths of all yarns in the unit cell together with dimensions and orientation of the yarn cross-section and the fibrous content values inside the yarn along the yarn path. A typical example in this

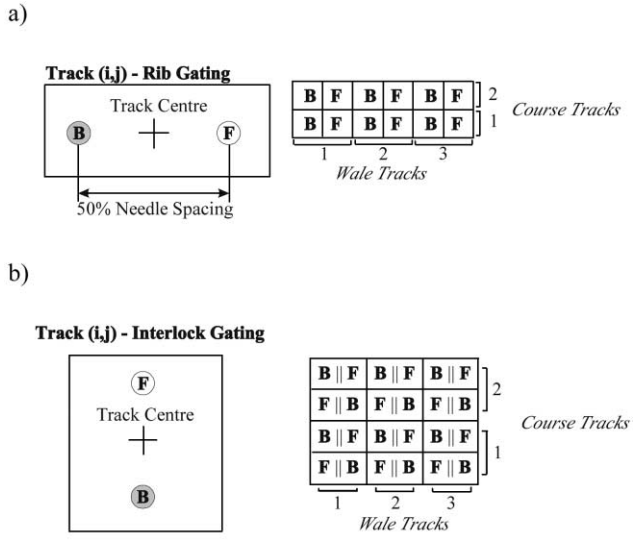

Fig. 7. Needle configuration for (a) the rib gating; (b) the interlock gating.

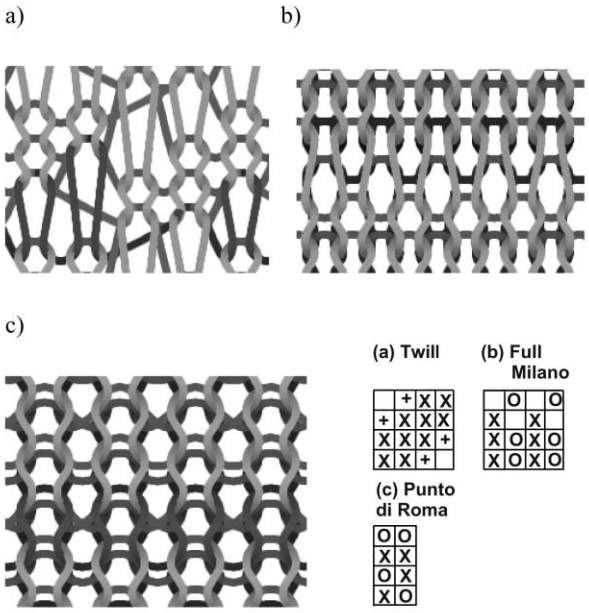

Fig. 8. Examples of interlacing patterns generated from topology coding (bottom right): (a) single jersey-(b) double jersey/rib gating and (c) double jersey/interlock gating.

category is the iso-strain based Fabric Geometry Model (FGM) [30]. It is also applicable to certain types of finite element models using 1D beam or truss idealisations, including, e.g. the Binary Model [30].

Analytical based models which use a mapping of an actual textile fibrous structure on a regular 3D mesh rely on another type of idealisation in order to reduce the model complexity. The idealisation consists of a volume discretisation in which the original textile architecture is mapped into a 3D grid of simpler, homogenised elements (voxel partitioning). Examples are found both in finite element modelling (mosaic type models) and the cell models described further. The TGP implements the *Fibre Distribution*

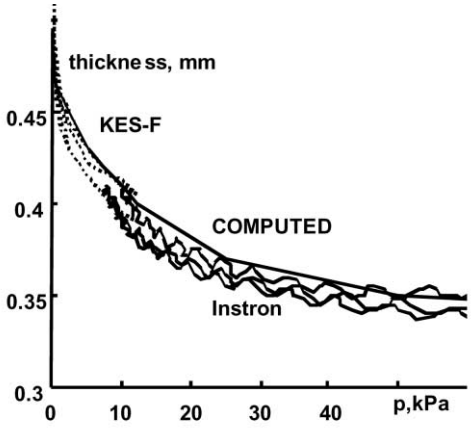

Fig. 9. Measured and computed compression curves of a glass reinforcement.

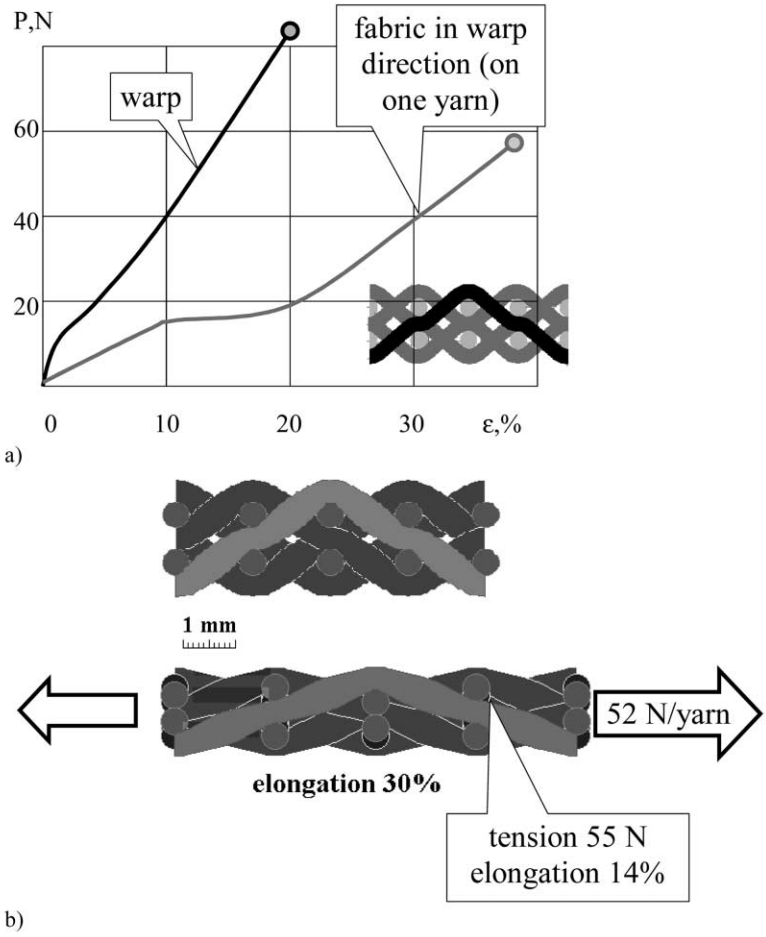

Fig. 10. Example of tensile test simulation for two-layered polyester fabric: (a) tension curve in the warp direction; (b) structure of the fabric under tension.

mode (FD) as an interface to this model class, creating a 3D array of data which stores fibre content and average fibre orientation for sub-cells of desired size.

At KULeuven, two types of meso-mechanical models which have been developed in the past and requiring the YP and FD interface are now briefly described.

5.1.1. YP mode

The first model is based on Eshelby's transformation concepts, and uses a short fibre analogy to describe the mechanical behaviour of curved yarn segments, combined with a Mori–Tanaka or self-consistent scheme [31,32] to account for interaction effects. The method has been described for knitted fabrics in Ref. [33], but the model description is generic and can be used for other textile types as well, provided that the yarn distribution within the unit cell is sufficiently 'fine'. The geometrical input consists of the yarn heart-line representations and cross-sectional dimensions. Yarns are split up into segments and replaced

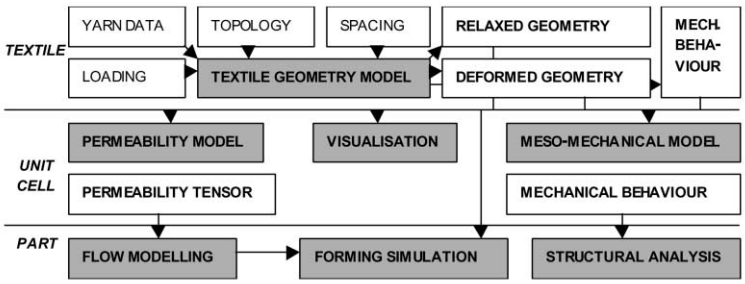

Fig. 11. Data flow for the integrated design tool.

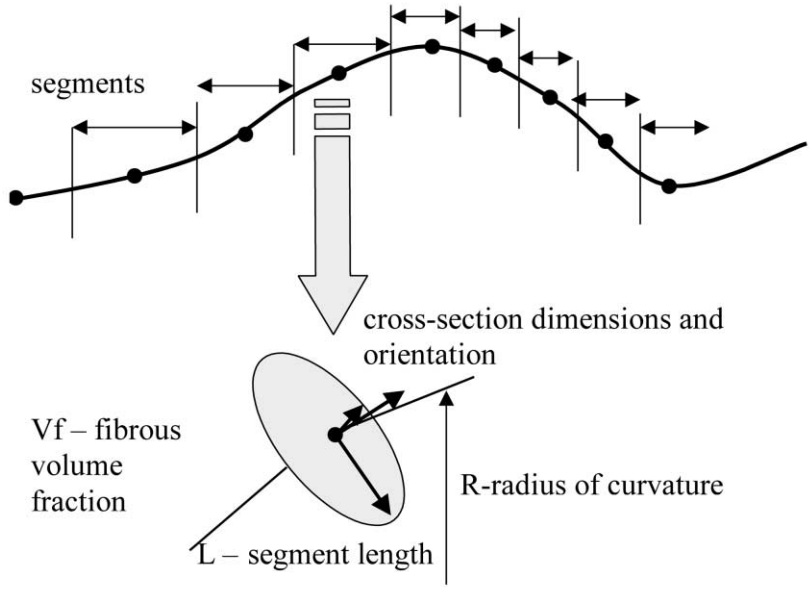

Fig. 12. TGP output in YP mode.

by a short fibre equivalent using the yarn orientation and the local curvature.

To accommodate these requirements, the following data are stored in the YP Mode (Fig. 12)

A. Repeat (unit cell) size.
B. Fibre data for all yarn types (fibre diameter, density, mechanical properties).
C. For each warp and weft yarn:
- yarn type reference;
- a sequence of data for consecutive segments on the yarn: segment length, radius of curvature, fibre volume fraction, cross-section size and orientation in the middle of the segment.

The number of segments is chosen by the user.

This data is ready available from the geometry description of a fabric, as described above.

The YP Mode output of TGP is processed by the meso-mechanical model as follows. First, for each yarn the description and the fibre data are read in. Next, for each yarn, the segment lengths, local fibre packing in the yarn, cross-sectional dimensions, curvature and local co-ordinate system are read in. Using the segment curvature as a parameter, each segment is mathematically represented in the meso-mechanical model by a short 'impregnated yarns' having an identical volume fraction, shape and orientation as the original yarn segment. Segment properties are calculated from the corresponding matrix and fibre properties and the local fibre packing in the segment, using an unidirectional Mori–Tanaka model. The final model is than solved with a classical Mori–Tanaka or self-consistent scheme.

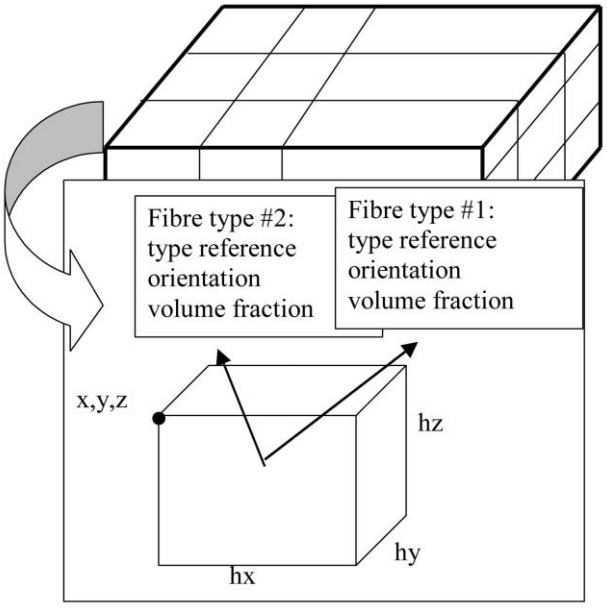

Fig. 13. TGP output in FD mode.

5.1.2. FD mode

The second model is a three-dimensional extension of Aboudi's method of cells [34]. The fabric repeat is mapped into an orthorombic, regular grid of cells, where each cell has homogenised properties according to the amount and respective orientations of the yarn sections it contains. The relationship between the macroscopic stress field and the local (homogenised) cell stresses is obtained as the solution of a complementary energy minimisation problem, subjected to stress continuity constraints across the cell interfaces. To limit the model size, the minimisation procedure is carried out on different length scales using

Table 3
Comparison of mechanical data for glass fabrics (Eshelby models)

Fabric	E_{WARP} (GPa)	E_{WEFT} (Gpa)	G_{XY} (GPa)	V_f (%)
R330-Experiment	16.9–25.7	18.7–22.5	3.8–4.4	36.8–44.7
R330-Eshelby model	20.0	20.1	3.4	39.1
R330-CEM model	19.8	20.0	3.3	
R420-Experiment	16.9–22.5	16.5–21.4	3.7–4.6	32.5–49.5
R420-Model	17.9	18.4	3.0	36.0
R420-CEM model	18.1	18.6	4.1	

sub-modelling techniques. A full treatment can be found in Ref. [35,36].

As an interface with this model, the following data are stored in the FD mode (Fig. 13)

A. Repeat (unit cell) size.
B. Data for all fibre types (fibre diameter, density, mechanical properties).
C. For each sub-cell:
- fibre type reference;
- average fibre orientation;
- average fibre volume fraction.

The number of sub-cells is chosen by the user.

Averaging over a sub-cell is done as follows. The geometrical model gives an answer to the question 'does a given point P in the unit cell volume lie inside a yarn?' If answer is *yes*, then the fibre volume fraction (from the fibre count inside the yarn and the cross-section compressed dimensions) and the fibre orientation (from yarn heart-line direction and yarn twist) can be computed for the point P. Integrating over a sub-cell volume, the average parameters are computed for each of fibre types present in the particular sub-cell

$$V_f = \frac{1}{V}\int_V v_f \, dv, \qquad \mathbf{A}_f = \frac{1}{V}\int_V \mathbf{a}_f \, dv, \tag{4}$$

where V is a subcell volume, v_f is fibre volume fraction (of fibres of the given type) near a given point P-centre of differential volume dv, $\mathbf{a}_f$ is fibre orientation vector at P, V_f is an average fibre volume fraction, $\mathbf{A}_f$ is an average fibre orientation (this vector is normalised after integration). Integrals are computed with a numerical formula

$$\int_V f \, dv \approx \sum_{i=1}^{n} \alpha_i f(P_i), \tag{5}$$

where n, coefficients α_i and reference points P_i inside a unit cell are pre-defined for a given polynomial order of accuracy (1,3,5 or 7, chosen by the user) [37].

5.1.3. Examples

Geometrical data generated by TGP have been used together with fibre and matrix mechanical data to calculate mechanical properties of composites.

5.1.3.1. 2D glass fabrics Consider composites produced in an autoclave from two glass fabrics (glass fibre properties $E = 72.0$ GPa, $\nu = 0.23$), using epoxy resin ($E = 3.0$ GPa, $\nu = 0.35$). For each fabric type, both composites with high (45–49%) and low (33–37%) volume fractions were produced. The difference is mainly in the resin layers between the fabric layers, but it will obviously affect in-plane elastic properties.

The experimental and calculated data are shown in Table 3. The experimental data shown are for low and high volume fractions. The calculated data are based upon the geometry and the volume fractions predicted by TGP using the dimensions of yarn cross-sections in the composite (compressed state). For the Eshelby models, only Mori–Tanaka predictions are shown, as they nearly coincide with self-consistent results for woven fabric textile composites [38]. Taking into account the predicted volume fraction, which is for most cases in between the experimental low- and high-volume fraction values, the correlation is very good.

5.1.3.2. 3D carbon fabric Mechanical properties of the fabric shown in Fig. 5 has been computed. The FGM-results for the fabric presented in Ref. [39] were used to back calculate neat fibre data. Available experimental and predicted data are summarised in Table 4. Predictions are all based on the TGP geometry using both an isostrain and self-consistent model (which for this type of materials again coincides closely with a Mori–Tanaka model). The fibre dominated E-moduli predictions are nearly identical for both models. However, Table 4 also indicates the well-known fact that FGM predicts systematically higher shear moduli [36]. The comparison with experimental data in Table 4 shows that at least the effect of the weaving geometry, noticeably the type and amount of Z-weaver yarns, is fairly well predicted.

5.2. Permeability models

The geometry of the reinforcement can be used to predict the permeability to resin flow. The permeability, K, governs the resin flow through the reinforcement during mould filling operations, such as resin transfer moulding [40], via

Table 4
Comparison of experimental data and model predictions with FGP: Iso-strain (FGM), Eshelby (self-consistent, SC) and Cell model (CEM)

	E_X	E_Y	E_Z	ν_{XY}	ν_{XZ}	ν_{YZ}	G_{YZ}	G_{XZ}	G_{XY}
Z3, measured	50.4	57.0	–	–	–	–	–	–	–
FGM	46.8	57.1	18.8	0.075	0.397	0.388	7.35	7.69	8.90
SC	48.7	56.0	15.8	0.082	0.346	0.322	4.94	5.16	7.84
CEM	47.9	56.4	16.2	0.083	0.366	0.342	5.14	5.38	8.10
Z6, measured	44.6	52.9	–	–	–	–	–	–	–
FGM	44.8	50.2	21.7	0.091	0.331	0.370	8.78	8.24	8.79
SC	44.1	50.2	19.1	0.092	0.290	0.310	5.94	5.51	7.36
CEM	45.1	51.9	20.8	0.10	0.311	0.320	6.02	5.84	7.50
Z9, measured	39.0	47.3	–	–	–	–	–	–	–
FGM	41.6	43.9	22.3	0.100	0.338	0.340	8.70	8.50	8.52
SC	40.2	43.2	20.6	0.103	0.282	0.293	5.88	5.87	6.78
CEM	40.5	43.8	21.2	0.150	0.302	0.309	5.93	5.90	6.81
Z12, measured	36.0	44.9	–	–	–	–	–	–	–
FGM	37.2	35.3	18.8	0.106	0.319	0.345	6.44	7.31	5.90
SC	35.7	33.9	17.3	0.103	0.297	0.276	3.78	4.97	4.33
CEM	36.1	34.2	17.9	0.151	0.310	0.303	3.86	5.01	4.41

Darcy's law,

$$v = -\frac{1}{\mu} K \nabla p,$$

where v is the superficial velocity, p is the pressure and μ is the fluid viscosity. A number of computer programs exist that solve Darcy's law and other relevant model equations to simulate the mould filling operation (see Ref. [41]), however, the availability of reliable values of K is critical to the success of such simulations. Available data, such as illustrated in Fig. 14, show the sensitivity of permeability to fibre architecture [42]. Note that at fibre volume fractions near 50%, the permeability may vary by over an order of magnitude, depending upon the fibre architecture.

Reliable measurements of permeability are difficult under relatively simple circumstances such as flat, undeformed geometry. In realistic circumstances such as curved geometry, and the various unsaturated flow conditions that occur during moulding, permeability values are nearly impossible to obtain.

A model able to predict, first, the yarn geometry in a draped fabric, and second, the permeability of the fabric would be valuable for process design and analysis. A new type of model, based on a lattice-Boltzmann approach [43], may be able to provide such predictive capability when linked to the fabric geometry model described above. The lattice-Boltzmann model solves for the detailed fluid flow within a unit cell of the reinforcement, and then integrates the computed fluid velocity distribution to generate a prediction of total flow at a prescribed pressure gradient. The predicted flow and prescribed pressure gradient are then combined with Darcy's law to provide a prediction of the permeability. When such predictions are generated for flows in different directions, the complete permeability tensor is generated for comparison to experiment. Although other numerical methods can, in principle, provide the same information, the lattice-Boltzmann method is particularly efficient for cases involving very complex geometry and multiphase flows, as found in resin transfer moulding.

The heterogeneous nature of the fibre reinforcements used in composites poses unique challenges for any numerical model since the very small pores between the filaments comprising each yarn would require extremely fine spatial discretisation if modelled in detail. The lattice-Boltzmann model being developed in this research is based, instead, on a hybrid description of the flow problem that mitigates the difficulty of fine spatial discretisation. Rather than treat the

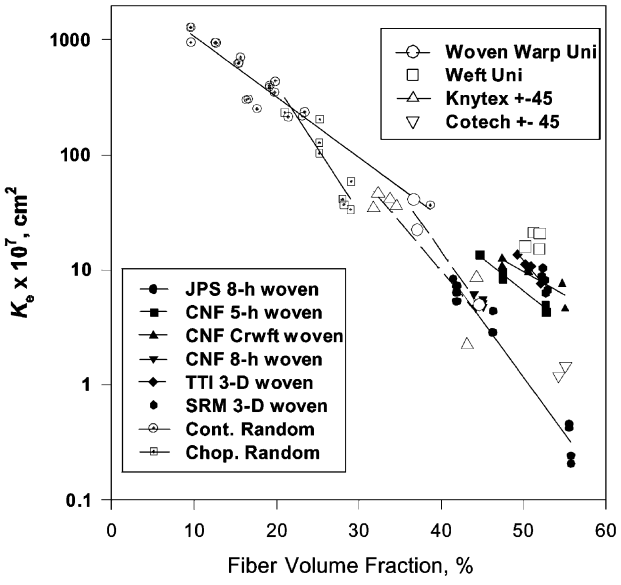

Fig. 14. In-plane permeability measurements for several glass fabrics indicate the importance of fibre architecture, in addition to volume fraction, in determining the permeability.

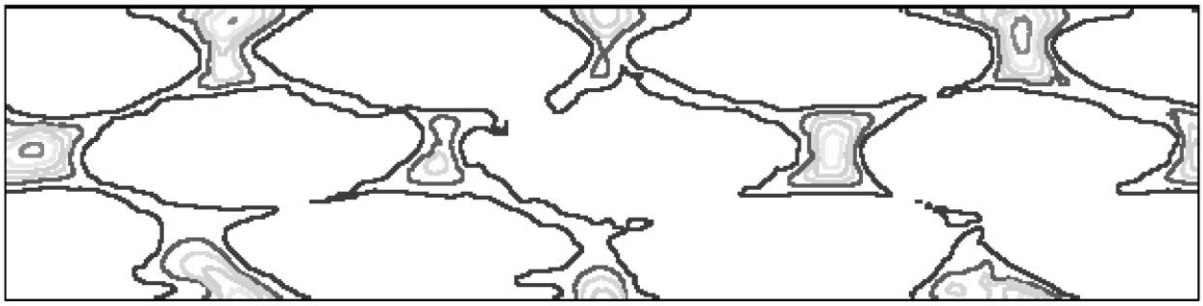

Fig. 15. Constant axial (yarns) velocity contours in the pores between yarns at a particular axial location within a warp knitted unidirectional glass fabric. Crossing threads do not appear in this particular slice, but are of critical importance in determining the total fluid flow. Figure originally published in Dunkers et al. (2001) [47].

micro-geometry inside the yarns in complete detail, the yarns are modelled as a small-scale porous medium using Brinkman's equation [44].

$$\nabla p = -\mu K^{-1} v + \mu \nabla^2 v$$

The larger scale of the yarn geometry and the porous structure between the yarns is modelled in detail, and the flow in the region between the yarns is described with Stokes equation,

$$\nabla p = \mu \nabla^2 v$$

The fluid velocity and gradient are matched at the boundary of the yarn and the open regions between the yarns to satisfy material and stress continuity.

Two early results illustrate the ability of the lattice-Boltzmann model to predict permeability. In one case, the fibre architecture of a warp knitted unidirectional glass reinforcement was obtained with non-destructive imaging [45], and the detailed fluid velocity distribution computed with the lattice-Boltzman model, as illustrated in Fig. 15. Lines of constant fluid velocity are shown in Fig. 15 in the larger porous regions between the yarns, but not within the yarns as the fluid velocities are very small within each yarn. Note the irregularity of the pore shapes and sizes. The computed permeability for flow in the fibre direction is in the range $(3.8–5.1) \times 10^{-10}$ m^2, while experimental results are in the range $(4.0–6.5) \times 10^{-10}$ m^2. Although these ranges appear large, note that the crossing threads are extremely important in determining the permeability, and removing them led to a 600% increase in the permeability of this particular material [46], both experimentally and computationally.

In the second case, the fabric geometry model discussed above was used to generate the fibre geometry of a plain-woven fabric at volume fractions ranging from 36–50%. At the lower volume fractions, the combined fabric geometry/lattice-Boltzmann model successfully predicted the permeability. For example, at $V_f = 37\%$, the experimental value for the permeability coefficient in the weft direction was 9.4×10^{-10} m^2, and the model prediction was 8.0×10^{-10} m^2. At higher fibre fractions, the combined models do not predict the permeability as well, and current work is refining the models by incorporating the irregularities apparent in Fig. 15.

6. Level IV: unit cell → composite part

When properties of a unit cell of composite material are known, predictions on the uppermost hierarchical level become possible using general purpose or specialised FE packages. As shown on Fig. 11, predictive models described above merge into an Integrated Design Tool, providing the long-waited solution for a designer of composite structures.

7. Conclusion

The modelling strategy proposed in the present work, provides a link between meso-mechanical and permeability models of composites and currently developed geometry models of textile reinforcement. It provides an opportunity to use manufacturer's fabric and yarns data, obtained on the standard equipment for textile testing, as a starting point for modelling of composite material. This gives more solid foundation for a priori predictions of mechanical properties of composites, allowing accounting for geometry peculiarities (complex crimp and porosity pattern) and yarn mechanical behaviour (compression) non-accessible in simple models. A 2D and 3D weave structure is easily constructed within TGP tools, providing great flexibility of input data. A user-friendly software application WiseTex allows easy manipulating of fabric and yarn data and visualisation tools. The model of the textile geometry and mechanics serves as a base for meso-mechanical and permeability models for composites, which provide therefore simulation tools for analysis of composites processing and properties. The critical hierarchical concept applies to many different types of textile reinforcement structures, resulting in integrated design software for textile composite modelling.

Acknowledgements

This work was done in the framework of the project Development of unified models for the mechanical behaviour of textile composites (GOA/98/05), funded by the Flemish Government through the Research Council of K.U. Leuven. S.V. Lomov's work on this project was supported by grants for Senior Fellowship by the Research Council of K.U. Leuven (F/98/108, F/99/096). Y. Luo work was supported by the Belgian program on Inter-university Poles of Attraction initiated by the Belgian State, Prime Minister's office, Science Policy Programming. R.S. Parnas's work was supported by the Fulbright Commission of the US State Department. Samples of woven reinforcements were supplied by Syncoglas, Belgium and TISSA, Switzerland. KES-F measurements were done in laboratories of Centexbel, Belgium, with kind permission and help of Dr E. Baetens and Dr D. Verstraete. Authors would also like to thank Prof. N.N. Truevtzev (St.-Petersburg State University of Technology and Design) for his constant support of international collaboration in the field of textile mechanics.

References

[1] Lomov SV, Gusakov AV, Huysmans G, Prodromou A, Verpoest I. Textile geometry preprocessor for meso-mechanical models of woven composites. Compos Sci Technol 2000;60:2083–95.
[2] Lomov SV, Huysmans G, Verpoest I. Hierarchy of textile structures and architecture of fabric geometrical models. Text Res J 2001 (in press).
[3] Prodromou AG, Ivens J, Huysmans G, Lomov S, Verpoest I. Stiffness and failure modelling of textile composites, ICCM-12 Conference, Paris, June 1999 (s.p.)
[4] Verpoest I, Lomov SV, Huysmans G, Ivens J. Modelling the processing and properties of textile composites: an integrated approach, 9th European Conference on Composite Materials Brighton, 2000 (s.p.)
[5] Lomov SV, Huysmans G, Luo Y, Prodromou A, Verpoest I, Gusakov AV. Textile Geometry Preprocessor for meso-mechanical and permeability modelling of textile composites, 9th European Conference on Composite Materials Brighton, 2000 (s.p.)
[6] Prodromou AG, Huysmans G, Lomov S, Ivens J, Verpoest I. A novel textile composites design and analysis tool. In: de Wilde WP, Blain WR, Brebbia CA, editors. Advances in composites materials and structures VII, Southampton, Boston: WIT press, 2000. p. 197–206.
[7] Lomov SV, Verpoest I. Integrated model of textile composite reinforcements. In: de Wilde WP, Blain WR, Brebbia CA, editors. Advances in composites materials and structures VII, Southampton, Boston: WIT Press, 2000. p. 367–76.
[8] Hearle JWS, Konopasek M, Newton A. On some general features of a computer-based system for calculation of the mechanics of textile structure. Text Res J 1972;42(10):613–26.
[9] Peirce FT. The geometry of cloth structure. J Text Inst 1937;28(3):T45–96.
[10] Pozdnyakov BP. Fabric resistance to tension in different directions. Moscow-Leningrad: GIZLegProm. 70, 1932 (in Russian)
[11] Novikov NG. A fabric structure and its design with the geometrical technique. Textilnaya Promishlennost 1946;6(2):9–17 (in Russian).
[12] Hearle JWS, Amirbayat J, Twaites JJ, editors. Mechanics of flexible fibre assemblies. Alphen aan den Rijn: Sijthoff and Nordhof, 1980.
[13] Parnas R, Phelan F. The effect of heterogeneous porous media on mold filling in resin transfer molding. SAMPE Q 1991;23(2):53–60.
[14] Hearle JWS, Shanahan WJ. An energy method for calculations in fabric mechanics. J Text Inst 1978;69(4):81–110.
[15] de Jong S, Postle R. A general energy analysis in fabric mechanics using optimal control theory. Text Res J 1978;48(3):127–35.
[16] Grishanov SA, Lomov SV, et al. The simulation of the geometry of two-component yarns. Part II. Fibre distribution in the yarn cross-section. J Text Inst 1997;88 part 1(4):352–72.
[17] Grishanov SA, Lomov SV, et al. The simulation of the geometry of two-component yarns. Part I. The mechanics of strand compression: simulating yarn cross-section shape. J Text Inst 1997;88 part 1(2):118–31.
[18] Lomov SV. Computer aided design of multilayered woven structures, part 1. Technologia Tekstilnoy Promyshlennosty 1993(1):40–5 (in Russian).
[19] Lomov SV. Prediction of geometry and mechanical properties of woven technical fabrics with mathematical modelling, Dept. Mechanical Technology of Fibrous Materials. SPbSUTD: St.-Petersburg, 1995.
[20] Lomov, SV, Truevtzev NN. A software package for the prediction of woven fabrics geometrical and mechanical properties. Fibres Text Eastern Eur 1995;3(2):49–52.
[21] Lomov SV, Verpoest I. Compression of woven reinforcements: a mathematical model. J Reinforced Plastics Compos 2000;19(16): 1329–50.
[22] Kawabata S, Niwa M, Kawai H. The finite-deformation theory of plain weave fabrics. Part I. The biaxial-deformation theory. J Text Inst 1973;64(1):21–46.
[23] Belov E, Lomov SV. Experimental investigation into loop forming (loss of stability) by turning of threads. Fibres Text Eastern Eur 1997;5(2):23–6.
[24] Belov EB, Lomov SV, Truevtzev NN, Bradshaw M, Harwood R. Measurement of the thread resistance to twisting and the critical snarl formation parameters. Chimicheskie Volokna 1999(3):37–41 (in Russian).
[25] Belov EB, Lomov SV, Truevtzev NN, Bradshaw M, Harwood R. On the problem of fancy yarn formation. Fibres Text Eastern Eur 1999;7(2):32–4.
[26] Gusakov AV, Lomov SV, Mogilny AN. Mathematical modelling of porosity of plane and 3D woven structures. In: Hoa SV, de Wilde WP, Bain WR, editors. Computer methods in composite materials VI. Southampton, Boston: Computational Mechanics Publications, 1998. p. 331–40.
[27] Lomov SV, Gusakov AV. Modellirung von drei-dimensionalen gewebe Strukturen. Technische Textilen 1995;38:20–1 (in German).
[28] Spencer DJ. Knitting technology. Cambridge: Woodhead Publishing, 1997.
[29] Lomov SV, Truevtzev AV. Computing an evaluation of bending rigidity ratio of a woven fabric and a yarn. Technologia Tekstilnoy Promyshlennosty 1994;N3:9–11 (in Russian).
[30] Cox BN, Carter WC, Fleck NA. A binary model of textile composites: I formulation. Acta Mater 1994;44(10):3463–79.
[31] Mura T. Micromechanics of defects in solids. Den Haag: Martinus Nijhoff Publishers, 1982.
[32] Mori T, Tanaka K. Average stress in matrix and average elastic energy of materials with misfitting inclusions. Acta Metall Mater 1973;21:571–4.
[33] Huysmans G, Verpoest I, Van Houtte P. A poly-inclusion approach for the elastic modelling of knitted fabric composites. Acta Mater 1998;46(9):3003–13.
[34] Aboudi J. Micromechanical analysis of composites by the method of cells. Appl Mech Rev 1989;42:193–221.
[35] Vandeurzen P. Structure-performance modelling of two-dimensional woven fabric composites, Dept MTM. Leuven: K.U. Leuven, 1998.
[36] Vandeurzen P, Ivens J, Verpoest I. Meso-stress analysis of woven

fabric composites by multilevel decomposition. J Compos Mater 1998;32(7):623–51.
[37] Krylov VI, Shulgina LT. Reference book for numerical integration. Moscow: Nauka, 1966 (in Russian).
[38] Huysmans G, Verpoest I, Van Houtte P. Eigenstrain models for complex textile composites. In: Proceedings of the Eighth European Conference on Composite Materials (ECCM-8), Naples, 1988;661–8.
[39] Gu, P. Analysis of 3D woven preforms and their composite properties. North Carolina State University, Raleigh, 1994;171.
[40] Parnas RS. Liquid Composite Molding. Hanser, 2000.
[41] Phelan FR. Simulation of the injection process in resin transfer molding. Polym Compos 1997;18(4):460–76.
[42] Parnas RS, Flynn KM, DalFavero ME. A permeability database for composites manufacturing. Polym Compos 1997;18(5):623–33.
[43] Spaid MAA, Phelan FR. Lattice Boltzmann methods for modeling microscale flow in fibrous porous media. Phys Fluids 1997; 9(9):2468–74.
[44] Phelan FR, Wise G. Analysis of transverse flow in aligned fibrous porous media. Composites 1996;27A(1):25–34.
[45] Dunkers JP, Parnas RS, Zimba CG, Peterson RC, Flynn KM, Fujimoto JG, Bouma BE. Optical coherence tomography of glass reinforced polymer composites. Composites: Part A 1999; 30:139–45.
[46] Phelan FR, Leung Y, Parnas RS. Modeling of microscale flow in unidirectional fibrous porous media. J Thermoplastic Compos Mat 1994;7:208–18.
[47] Dunkers JP, Phelan FR, Zimba CG, Flynn KM, Sanders DP, Peterson RC, Parnas RS, Li X, Fujimoto JG. The prediction of permeability for an epoxy/E-glass composite using optical coherence tomography images. Polym Compos 2001 (in press).